

# Orthogonality Effects in Relativistic Models of Nucleon Knockout Reactions\*

**J.I. Johansson and H.S. Sherif**

Department of Physics, University of Alberta  
Edmonton, Alberta, Canada T6G 2J1

and

**F. Ghoddoussi**

Department of Physics, University of Alberta  
Edmonton, Alberta, Canada T6G 2J1

and

Department of Physics and Astronomy  
Wayne State University  
Detroit, Michigan, USA 48202

February 7, 2020

## Abstract

We study the effect of wave function orthogonality in the relativistic treatment of the nucleon removal reactions  $(\gamma, p)$  and  $(e, e'p)$ . The continuum wave function describing the outgoing nucleon is made orthogonal to the relevant bound states using the Gram-Schmidt procedure. This procedure has the advantage of preserving the asymptotic character of the continuum wave function and hence the elastic observables are unaffected. The orthogonality effects are found to be

---

\*This work is supported in part by the Natural Sciences and Engineering Research Council of Canada

negligible for  $(e, e'p)$  reactions for missing momenta up to  $700 \text{ MeV}/c$ . This holds true for both parallel and perpendicular kinematics. By contrast the orthogonalization of the wave functions appears to have a more pronounced effect in the case of  $(\gamma, p)$  reactions. We find that the orthogonality effect can be significant in this case particularly for large angles. Polarization of the outgoing protons and photon asymmetry show more sensitivity than the cross sections. If the orthogonality condition is imposed solely on this one hole state the effects are usually smaller.

# 1 Introduction

Nucleon removal reactions play a central role in clarifying important aspects of the nature of nuclear states, particularly those related to the shell structure of nuclei. There is currently renewed interest in these reactions when the probe is electromagnetic as more sophisticated electron beam machines are now available. The new generation of possible experiments opens the door to more precise and elaborate data that will help us understand the intricacies of the reaction mechanism and look at possible changes in the structure of nucleons and other hadrons as they move within the nuclear environment. Spin dependent observables are expected to play a key role in these investigations.

Most earlier analyses of reactions such as the quasielastic  $(e, e'p)$  and  $(\gamma, p)$  reactions have been carried out using the non-relativistic distorted wave impulse approximation (NRDWIA) [1, 2]. In this approach the nucleon wave functions needed for the calculation of the reaction amplitude are solutions of the Schrödinger equation, and the current operators are obtained from the free probe-nucleon relativistic amplitude via some non-relativistic reduction scheme [3]. Recently however it has become clear that a fully relativistic approach to the description of these reactions is more appropriate [4, 5, 6, 7, 8, 9, 10]. This is evidenced by the improvement in the values of the spectroscopic factors obtained using this approach and indications of improvements to recoil polarization [11, 12] as well as cross sections at large missing momenta [13].

Because of the expectation that more precise and expanded data will become available shortly, there has been concentrated activity aimed at discerning details of the theoretical calculations of the amplitudes. The interplay between relativistic and non-relativistic approaches has been studied by several authors, and recently aspects of gauge dependence as well as coupling effects have been investigated [14, 15].

The purpose of the present paper is to address one detail of the calculations of the amplitudes which is usually overlooked: namely, both relativistic and non-relativistic DWIA versions of the amplitude for a variety of reactions, including  $(e, e'p)$  and  $(\gamma, p)$  (which are the focus of the present study) suffer from an orthogonality defect. These distorted wave models utilize wave functions for bound and continuum states, which are solutions of equations containing different hamiltonians; the bound states are generated from real potentials, while the continuum states are generated from complex en-

ergy dependent optical potentials. The character of the latter potentials is dictated by the need to account for nucleon elastic scattering observables. The wave functions are therefore not orthogonal, in contradiction to what a fundamental theory would require.

The impact of the nonorthogonality defect has been discussed in the past and ways to remedy it have been suggested [16, 17, 18, 19, 20, 21, 22, 23]. The majority of these discussions were done in a non-relativistic framework but many of the remedies suggested have never been utilized in main stream calculations. Noble [17] attempted to recast the amplitude for photoabsorption into a form that takes into account the orthogonality of the nucleon wave functions. Difficulties with this approach have been discussed by Eisenberg, Noble and Weber [18]. Celenza and Shakin [19] suggested that a modified hamiltonian for the continuum states can be constructed in such a manner as to guarantee both orthogonality with the bound states, and a fit to the proton elastic scattering data. This proposition was never tested in practice. Other possibilities discussed by Boffi *et al.* [21, 22] involved the introduction of effective operators, but it turned out that these were too difficult to calculate.

For the two reactions under consideration, however, a more practical approach was identified and used to assess the role of non-orthogonality on the non-relativistic amplitudes. It was suggested by Boffi *et al.* [21, 22] as well as by Ciofi Degli Atti *et al.* [20] that the continuum states can be made orthogonal to the bound states by applying a Gram-Schmidt orthogonalization procedure. In the present work we use this same method to examine the importance of orthogonalization in the relativistic approach to nucleon knockout reactions.

In the following text we give a brief outline of the relativistic calculations for nucleon knockout induced by the quasi elastic scattering of electrons or the absorption of real photons. We then introduce the method of orthogonalization of the nucleon wave functions and calculate the resulting corrections to the reaction amplitude. A discussion of the impact of these changes on the reaction observables is given in section 3. We conclude in section 4.

## 2 The Relativistic Calculations

The relativistic calculations of the amplitude, in the one photon exchange model for the  $(e, e'p)$  process, are discussed in Refs. [4, 5, 6, 7, 8]. Relativistic

calculations for  $(\gamma, p)$  reactions are discussed in Refs. [5, 9, 10]. It is sufficient for the purpose of the present discussion to focus on the nuclear matrix element portion of the amplitude, which can be written in a unified form for reactions involving either virtual or real photons. In the notation of Ref. [5] the relativistic expression for the nuclear matrix element  $N_\beta^{\mu M_B}$ , leading to a specific final state of the residual nucleus for both the  $(\gamma, p)$  and  $(e, e'p)$  reactions can be written as

$$N_\beta^{\mu M_B} = \int d^3r \left[ \Psi_\mu^{(-)} \right]^\dagger (\mathbf{p}, \mathbf{r}) \Gamma_\beta \Psi_{J_B, M_B}(\mathbf{r}) \exp(i\mathbf{q} \cdot \mathbf{r}), \quad (1)$$

where  $M_B$  and  $\mu$  are the spin projections of the bound and continuum nucleons, respectively, and  $\mathbf{p}$  is the 3-momentum of the latter. The  $4 \times 4$  matrix  $\Gamma_\beta$ , operating on the nucleon spinors, is given in detail for the  $(e, e'p)$  reaction, in Eq. (2.8) of reference [4]. For the  $(\gamma, p)$  reaction,  $\Gamma_\beta$  is written explicitly in Ref. [24].

In relativistic DWIA (RDWIA) calculations of the amplitude,  $\Psi_\mu$  is chosen as the Dirac continuum wave function in the elastic channel. It is generated by using a complex nucleon-nucleus optical potential, and is required to give an acceptable account of the elastic data. The spinor  $\Psi_{J_B, M_B}$ , on the other hand, is a solution of the bound state Dirac equation, which contains real scalar and vector potentials. It is clear then that the nucleon wave functions used in the RDWIA are not orthogonal since they are solutions of the Dirac equation for two different hamiltonians. It is the lack of orthogonality of the spinors  $\Psi_\mu$  and  $\Psi_{J_B, M_B}$  that is the subject of the present study.

## 2.1 Orthogonal States

The orthogonal continuum wave function is obtained via the Gram-Schmidt method. This involves subtracting a multiple of the bound state wave functions for each of the occupied levels of the target nucleus. The approach has the advantage of being easily incorporated within the RDWIA approach as a means of gaining some insight into the possible corrections arising from the orthogonality defect. The proposed orthogonal wave function can be written in terms of the original distorted wave and the bound state wave functions as

$$\tilde{\Psi}_\mu^{(+)}(\mathbf{p}, \mathbf{r}) = \Psi_\mu^{(+)}(\mathbf{p}, \mathbf{r}) - \sum_{L'_B, J'_B, M'_B} \beta_\mu^{L'_B, J'_B, M'_B} \Psi_{L'_B, J'_B, M'_B}(\mathbf{r}), \quad (2)$$

where the sum is over all the occupied bound states (characterized here by their angular momentum labels  $L'_B, J'_B, M'_B$ ). Note that the coefficient,  $\beta_\mu^{L'_B, J'_B, M'_B}$ , in the second term of Eq. (2) is required to have the same asymptotic spin projection  $\mu$ , as the original continuum wave function.

It was shown by Ciofi Degli Atti *et al.* [20] that there is a close connection between the above form of orthogonalized wave functions and the requirement of antisymmetrization of the final state wave function in reactions initiated by the real photons. A crucial advantage of the above prescription is that the resulting orthogonal continuum wave functions continue to yield the same proper description of elastic scattering provided by the original proton continuum wave function.

The expansion coefficients  $\beta_\mu^{L'_B, J'_B, M'_B}$  are determined by requiring that the wave function given in Eq. (2) is orthogonal to all occupied states of the target; this yields

$$\beta_\mu^{L_B, J_B, M_B} = \langle \Psi_{L_B, J_B, M_B}(\mathbf{r}) | \Psi_\mu(\mathbf{p}, \mathbf{r}) \rangle. \quad (3)$$

The detailed evaluation of these expansion coefficients requires the standard partial wave expansion for the wave functions. For the continuum state we write

$$\begin{aligned} \psi_\mu^{(+)}(\mathbf{p}, \mathbf{r}) &= 4\pi \left[ \frac{E_N + m_N}{2m_N} \right]^{1/2} \\ &\sum_{LJM} i^L [Y_L^{M-\mu}(\hat{\mathbf{p}})]^* (L, 1/2; M - \mu, \mu | J, M) \\ &\times \left[ \begin{array}{c} f_{LJ}(r) \\ -ig_{LJ}(r) \boldsymbol{\sigma} \cdot \hat{\mathbf{r}} \end{array} \right] \mathcal{Y}_{L \frac{1}{2} J}^M(\hat{\mathbf{r}}). \end{aligned} \quad (4)$$

where the upper and lower component radial functions,  $f_{LJ}(r)$  and  $g_{LJ}(r)$ , are solutions of equations containing complex scalar and vector potentials. For the bound state with angular momentum quantum numbers  $L_B, J_B, M_B$  we can write

$$\Psi_{J_B, M_B}(\mathbf{r}) = \left[ \begin{array}{c} f_{L_B J_B}(r) \\ -ig_{L_B J_B}(r) \boldsymbol{\sigma} \cdot \hat{\mathbf{r}} \end{array} \right] \mathcal{Y}_{L_B \frac{1}{2} J_B}^{M_B}(\hat{\mathbf{r}}). \quad (5)$$

Using Eqs. (4) and (5) in Eq. (3), we get for the expansion coefficients

$$\begin{aligned} \beta_\mu^{L_B, J_B, M_B} &= 4\pi \left[ \frac{E_N + m_N}{2m_N} \right]^{1/2} (L_B, 1/2; M_B - \mu, \mu | J_B, M_B) \\ &[Y_{L_B}^{M_B - \mu}(\hat{\mathbf{p}})]^* b_{L_B, J_B}. \end{aligned} \quad (6)$$

where  $b_{L_B, J_B}$  is the overlap integral between the bound and distorted wave radial functions:

$$b_{L_B, J_B} = \int r^2 dr \left[ f_{L_B J_B}^{(bound)}(r) f_{L_B J_B}^{(cont)}(r) + g_{L_B J_B}^{(bound)}(r) g_{L_B J_B}^{(cont)}(r) \right]. \quad (7)$$

Using Eqs. (4) and (6) in Eq. (2) allows us to write a partial wave expansion for the distorted wave which will be orthogonal to the bound states. The result is that the continuum wave function is changed only in partial waves with angular momentum quantum numbers corresponding to the occupied levels of the target nucleus. The resulting continuum wave function is suitable for use in calculations of the nuclear matrix element of Eq. (1) without further modification, and is straightforward to include in existing reaction codes.

### 3 Discussion

To assess the impact of the wave function nonorthogonality in realistic situations we have carried out calculations for a number of cases involving photonuclear knockout of protons for photon energies above 60 MeV. We also extend the study to electron quasielastic scattering on the same nuclei. In these calculations we use bound state wave functions which are generated using phenomenological Dirac scalar and vector potentials with Woods-Saxon shapes. The parameters of the potentials are determined by the requirement that the separation energies of the states for which we have experimental data are reasonably well reproduced. This binding potential is used to generate the entire family of occupied states in the target. The distorted waves are generated using the energy dependent potentials of Cooper *et al.* [25]. For the  $^{16}\text{O}$  target we use the energy-dependent potentials specific to this target (EDAI O16), while for the other nuclei considered we use the energy- and mass-dependent set (EDAD Fit 1) These distorted wave functions are then made orthogonal to the family of bound states following the procedure discussed in section 2.

The size of the orthogonality effect is linked to the magnitude of the coefficients  $b_{L_B, J_B}$  given in Eq. (7). As is seen from this equation, the coefficients are radial overlaps between bound and continuum wave functions. Figure 1 shows the behavior of the overlap coefficient for the  $1p_{1/2}$  state in  $^{16}\text{O}$  as a function of the energy of the continuum nucleon. Part (a) of the figure shows

the real (solid) and imaginary (dashed) parts of the coefficient on a standard plot, while part (b) shows the absolute value of the real and imaginary parts on a semilogarithmic plot. As one might expect these overlap coefficients are larger at lower energies and drop quickly as the energy increases. They have oscillatory behavior reflecting that particular character of the continuum radial wave functions. At low energies ( $\approx 10$  MeV) the magnitude of the coefficients can be close to 0.1. Although these are relatively large, they are not likely to have large effects in the energy region of interest for the reactions under consideration. Note also that the orthogonality requirement affects only a limited number of partial waves (depending on the target nucleus) in the continuum wave function: those corresponding to occupied states in the target nucleus.

In the present work, the effects of orthogonality are studied in two cases:

- i) *Minimal orthogonality*: the continuum wave function is made orthogonal to only the one-hole state involved in the reaction;
- ii) *Full orthogonality*: the continuum wave function is made orthogonal to all occupied states of the target.

In the following we give an account of the results obtained for the two reactions under consideration.

### 3.1 $(\gamma, p)$ Reactions:

We have investigated the effect of non-orthogonality on the cross section, proton polarization and photon asymmetry in  $(\gamma, p)$  reactions on four nuclei:  $^{12}\text{C}$ ,  $^{16}\text{O}$ ,  $^{40}\text{Ca}$  and  $^{208}\text{Pb}$ , for photon energies from 60 to 500 MeV. Two representative examples of these calculations are shown in Figs. 2 and 3. In Fig. 2 we show the calculations for the reaction  $^{16}\text{O}(\gamma, p)$  at an incident photon energy of  $E_\gamma = 100$  MeV. A proton is removed from the  $1p_{1/2}$  level and the residual nucleus is left in the ground state. In Fig. 3 we show similar calculations for incident photon energy  $E_\gamma = 196$  MeV. To put the comparisons in a proper context we also show the experimental cross section data for the above reactions [26, 27].

We note that the effects of minimal orthogonalization are generally smaller than those for full orthogonalization. The cross sections (part (a) of the figures) are affected only slightly at most angles but the deviations can be large at extreme backward angles. The relative increase of the effect at large angles



is a reflection of the fact, mentioned above, that the orthogonality requirement modifies only low partial waves. The effects on proton polarization (part (b)) and photon asymmetry (part (c)) are noticeable over most of the angular range, but are small at the very forward angles. This is an indication that these two observables are somewhat more sensitive to the orthogonality defect than are the cross sections.

Figures 4 and 5 shed more light on the role of orthogonality and the dependence on the photon energy and the angle of the outgoing protons. Here we show the photon energy dependence of the cross section on  $^{40}\text{Ca}$  at proton angles of  $\theta_p = 90^\circ$  (Fig. 4) and  $\theta_p = 135^\circ$  (Fig. 5). The cross section data shown in both figures are from Leitch *et al.* [28]. We observe from Fig. 4 that at  $\theta_p = 90^\circ$  the effects on the direct knockout cross section are rather small up to photon energies of 300  $\text{MeV}$  (calculations show this feature still prevails at higher energies). At  $\theta_p = 135^\circ$  (Fig. 5), we find larger effects on the cross section, particularly when full orthogonalization is imposed on the wave functions. These results are in qualitative agreement with the observations made by Ciofi Degli Atti *et al.* [20] using the non-relativistic approach. Parts (b) and (c) of the figures show the effects on proton polarization and photon asymmetry, respectively. Here we note large effects on both observables at both angles and over the entire energy range (these effects are much smaller at  $\theta_p = 45^\circ$ ). It is evident that the spin observables are more sensitive to the orthogonality of the wave functions.

Boffi *et al.* [21, 22] argued that the effect of non-orthogonality on the unfactorized  $(\gamma, p)$  cross sections vanishes because of the transverse nature of the electromagnetic current. Our present calculations do not support this conclusion; as seen in the preceding figures, we do observe some effects when using only minimal orthogonalization. The reason for the difference is that in Eq. (2), even if one restricts the sum to a single orbital  $(L_B, J_B)$  there are still contributions from different magnetic substates. As a result some of the contributions from orthogonalization do not vanish. This difference can be stated as due to the possibility of spin-flip in the outgoing channel (which is closely linked to the presence of the spin-orbit interaction); such a possibility was not taken into account by Boffi *et al.*

Earlier estimates of the orthogonality effects in  $(\gamma, p)$  reactions were obtained for non-relativistic calculations by Fink *et al.* [23] and for relativistic calculations by Lotz [29]. The procedure followed was to replace the distorting potential of the continuum proton with the bound state potential. The continuum and bound state hamiltonians are thus identical and hence

the wave functions are orthogonal. The dotted curve in Fig. 4 shows the calculated observables when this procedure is implemented. The effects are seen to be much more exaggerated in this case. It should be noted that one important shortcoming of this procedure is that the new distorted wave function is no longer able to reproduce the elastic scattering data. This difficulty is also present in non-relativistic calculations that use continuum RPA wave functions [30].

### 3.2 $(e, e'p)$ Reactions:

We have also carried out similar calculations for the  $(e, e'p)$  reaction. Boffi *et al.* [21, 22] and Ciofi Degli Atti *et al.* [20] have reported that in the non-relativistic calculations of the amplitudes the orthogonalization effects are quite small. Our relativistic calculations confirm this conclusion. We have carried out calculations for electron energies of 460 *MeV* and 2.4 *GeV* and found that the spectral functions are affected only slightly by the imposition of orthogonality. Our calculations covered missing momenta in the range  $\pm 700$  *MeV/c*. At proton energies of 100 *MeV* or higher the effects of orthogonality are essentially negligible. At low proton kinetic energies we find some orthogonality effects in the proton polarization calculations. Figure 6 shows calculations for the reaction  $^{16}\text{O}(e, e'p)$  in perpendicular kinematics with a proton energy of  $T_p = 35$  *MeV*. It is evident in this figure that orthogonality effects are small except at the large missing momenta. Figure 7 shows quasifree electron scattering calculations for the  $^{40}\text{Ca}$  target in parallel kinematics, with a proton energy of  $T_p = 100$  *MeV*. The orthogonality corrections due to Eq. (2) are negligible, but replacing the distorting potential with the binding potential, as was done in Fig. 4, has a large effect. This prescription cannot be advocated because the distorted wave is no longer able to describe proton elastic scattering. Note that these latter calculations cannot describe the electron scattering data very well either.

## 4 Conclusion

In this paper we have investigated the role of wave function orthogonality in relativistic calculations of  $(\gamma, p)$  and  $(e, e'p)$  reactions. We have used a Gram-Schmidt procedure [21, 22, 20] to orthogonalize the continuum and bound-state wave functions of the nucleon. This procedure, besides being

closely linked to the antisymmetrization [20] of the final state wave function, also has the merit of leaving the continuum wave function asymptotically intact. This ensures that the wave function continues to provide the same good description of the elastic scattering data as the original distorted wave. Calculations were carried out for two schemes, one where orthogonality is imposed only in relation to the specific hole state involved in the reaction, and full orthogonality with all occupied levels. The effects in the latter case were found to be larger.

The present study suggests that the orthogonality effects are not a serious problem for  $(e, e'p)$  reactions. Calculations over a wide range of missing momenta do not show large deviations from the traditional nonorthogonal calculations except for the spin dependent observables at large missing momenta.

The orthogonality effects are found to be non-negligible in the case of  $(\gamma, p)$  reactions. Our calculations show that these effects tend to be more pronounced at large angles of the outgoing protons. The spin observables appear to be more sensitive to the orthogonality of the wave functions. This may have important ramifications for calculations of the amplitudes for higher order processes such as those associated with two-nucleon currents.

## References

- [1] D.G. Ireland and G. van der Steenhoven, Phys. Rev. C **49** (1994) 2182, and references therein.
- [2] L. Lapikas, J. Wesseling and R. B. Wiringa, Phys. Rev. Lett. **82** (1999) 4404, and references therein.
- [3] K.W. Mcvoy and L.Van Hove, Phys. Rev. **125** (1962) 1034.
- [4] M. Hedayati-Poor, J.I. Johansson and H.S. Sherif, Phys. Rev. C **51** (1995) 2044.
- [5] J.I. Johansson and H.S. Sherif, Nucl. Phys. **A605** 517 (1996).
- [6] J.M. Udias, P. Sarriguren, E. Moya de Guerra, E. Garrido and J.A. Caballero, Phys. Rev. C **48** (1993) 2731.
- [7] J.M. Udias, P. Sarriguren, E. Moya de Guerra, E. Garrido and J.A. Caballero, Phys. Rev. C **51** (1995) 3246.
- [8] Yanhe Jin and D.S. Onley, Phys. Rev. C **50** (1994) 377.
- [9] G.M. Lotz and H.S. Sherif, Phys. Lett. B **210** (1988) 45; and Nucl. Phys. **A537** (1992) 285.
- [10] J.I. Johansson, H.S. Sherif and G.M. Lotz, Nucl. Phys. **A605** (1996) 517.
- [11] J.I. Johansson and H.S. Sherif, in: *SPIN96 Proceedings*, edited by C.W. de Jager, T.J. Ketel, P.J. Mulders, J.E.J. Oberski and M. Oskam-Tamboezer (World Scientific, Singapore, 1997), p. 377.
- [12] J.I. Johansson and H.S. Sherif, Phys. Rev. C **59** (1999) 3481.
- [13] J.M. Udias, P. Sarriguren, E. Moya de Guerra and J.A. Caballero, Phys.Rev. C **53** (1996) 1488
- [14] James J. Kelly, Phys.Rev. C **56** (1997) 2672.
- [15] James J. Kelly, Phys.Rev. C **59** (1999) 3256.
- [16] R.D. Amado and R. Woloshyn, Phys. Lett. **69B** 400 (1977).

- [17] J.V. Noble, Phys. Rev. C **17** (1978) 2151.
- [18] J.M. Eisenberg, J.V. Noble and H.J. Weber, Phys. Rev. C **19** (1979) 276.
- [19] Louis S. Celenza and C. M. Shakin, Phys.Rev. C **20** (1979) 385.
- [20] C. Ciofi Degli Atti, M.M. Giannini and G. Salmè, Il Nuovo Cimento **76A** (1983) 225.
- [21] S. Boffi, F. Cannata, F. Capuzzi, C. Giusti and F.D. Pacati, Nuclear Physics **A379** (1982) 509.
- [22] S. Boffi, Il Nuovo Cimento **76A** (1983) 186.
- [23] M. Fink, H. Hebach and H. Kümmel, Nucl. Phys. **A186** (1972) 353.
- [24] J.I. Johansson and H.S. Sherif, Phys. Rev. C **56** (1997) 328.
- [25] E.D. Cooper, S. Hama, B.C. Clark and R.L. Mercer, Phys. Rev. C **47** (1993) 297.
- [26] D.J.S. Findlay and R.O. Owens, Nucl. Phys. **A279** (1977) 385.
- [27] G.S. Adams *et al.* Phys Rev C 38 (1988) 2771.
- [28] M.J. Leitch, F.C. Lin, J.L. Matthews, W.W. Sapp, C.P. Sargent, D.J.S. Findlay, R.O. Owens and B.L. Roberts, Phys. Rev. C **33** (1986) 1511.
- [29] G.M. Lotz, Ph.D. thesis University of Alberta (1989).
- [30] V. Van der Sluys, J. Ryckebusch, and M. Waroquier, Phys. Rev. C **54** (1996) 1322.
- [31] G.J. Kramer *et al.*, Phys. Lett. B **227** (1989) 199.

## Figure Captions

FIG. 1. The overlap coefficients,  $b_{L_B, J_B}$ , of Eq. (7) for the  $1s_{1/2}$  state in the  $^{16}\text{O}$  target. The binding potentials have Woods-Saxon shapes, while the proton optical potentials are the E-dependent optical potential for  $^{16}\text{O}$  from Ref. [25]. (a) linear plot of real (solid) and imaginary (dashed) parts, and, (b) semilogarithmic plot of absolute value of real (solid) and imaginary (dashed) parts.

FIG. 2. Effect of wave function orthogonalization in the  $^{16}\text{O}(\gamma, p)^{15}\text{N}_{g.s.}$  reaction involving the knockout of a  $1p_{1/2}$  proton. The energy of the incident photon is  $100\text{ MeV}$ . The binding potentials have Woods-Saxon shapes, while the proton optical potentials are the E-dependent optical potentials for  $^{16}\text{O}$  from Ref. [25]. (a) Cross section. (b) Proton polarization. (c) Photon asymmetry. Solid curves — no orthogonality. Long-dashed curves — minimal orthogonality. Short-dashed curves — full orthogonality. The data are from Ref. [26].

FIG. 3. Same as Fig. 2, except the energy of the incident photon is  $196\text{ MeV}$ . The data are from Ref. [27].

FIG. 4. Effect of wave function orthogonalization in the  $^{40}\text{Ca}(\gamma, p)^{39}\text{K}_{g.s.}$  reaction involving the knockout of a  $1d_{3/2}$  proton. The angle of the final proton is  $90^\circ$ . The binding potentials have Woods-Saxon shapes, while the proton optical potentials are E- and A-dependent optical potentials (Fit 1) from Ref. [25]. (a) Cross section. (b) Proton polarization. (c) Photon asymmetry. Solid curves — no orthogonality. Long-dashed curves — minimal orthogonality. Short-dashed curves — full orthogonality. Dotted curves — continuum wave function calculated using binding potential. The data are from Ref. [28].

FIG. 5. Same as Fig. 4, except the angle of the final proton is  $135^\circ$ . The data are from Ref. [28].

FIG. 6. Effect of wave function orthogonalization in the  $^{16}\text{O}(e, e'p)^{15}\text{N}_{g.s.}$  reaction involving the knockout of a  $1p_{1/2}$  proton. The energy of the incident electron is  $456\text{ MeV}$ , with perpendicular kinematics, and the proton kinetic energy is  $T_p = 35\text{ MeV}$ . The binding potentials have Woods-Saxon shapes, while the proton optical potentials are the E-dependent optical potentials

for  $^{16}\text{O}$  from Ref. [25]. (a) Cross section. (b) Proton polarization. Solid curves — no orthogonality. Long-dashed curves — minimal orthogonality. Short-dashed curves — full orthogonality.

FIG. 7. Effect of wave function orthogonalization in the  $^{40}\text{Ca}(e, e'p)^{39}\text{K}_{g.s.}$  reaction involving the knockout of a  $1d_{3/2}$  proton. The energy of the incident electron is  $460\text{ MeV}$ , with parallel kinematics, and the proton kinetic energy is  $T_p = 100\text{ MeV}$ . The binding potentials have Woods-Saxon shapes, while the proton optical potentials are E- and A-dependent optical potentials (Fit 1) from Ref. [25]. (a) Cross section. (b) Proton polarization. Solid curves — no orthogonality. Long-dashed curves — minimal orthogonality. Short-dashed curves — full orthogonality. Dotted curves — continuum wave function calculated using binding potential. The data are from Ref. [31].

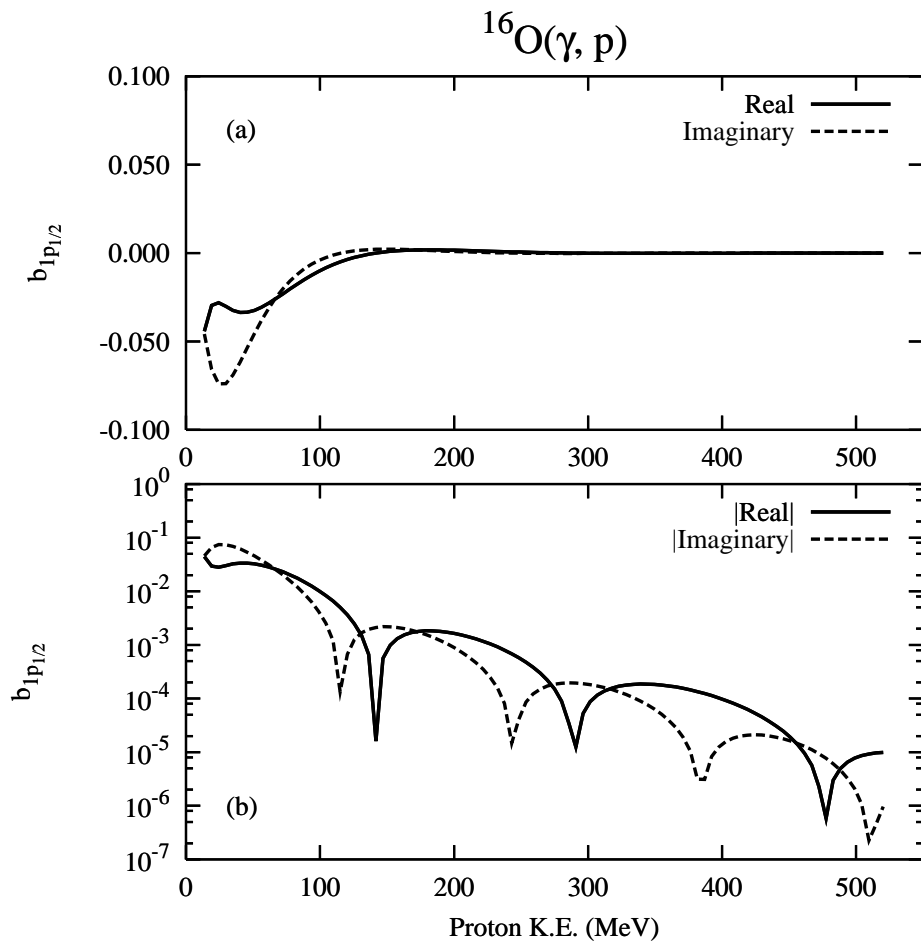


FIGURE 1



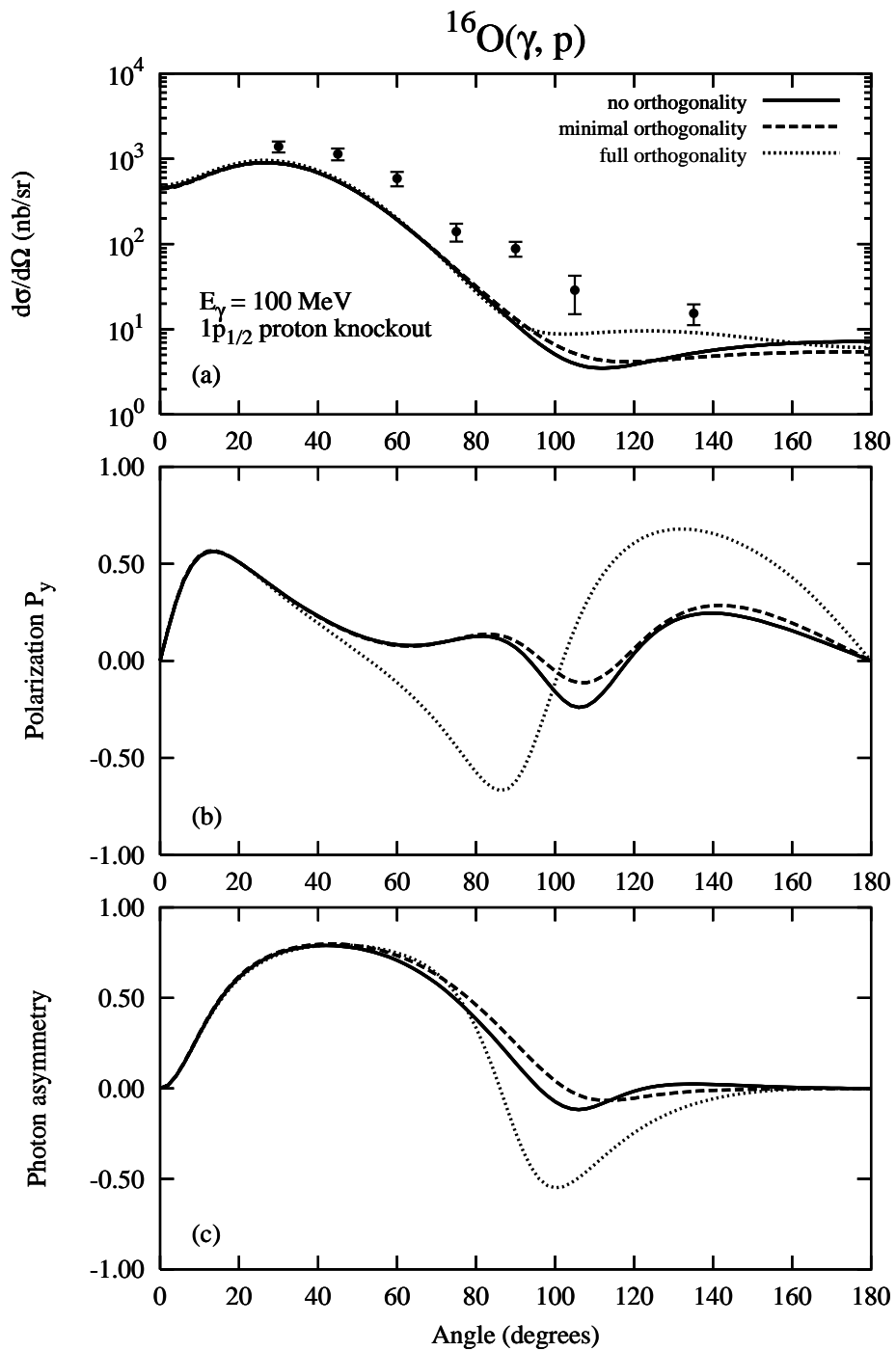


FIGURE 2

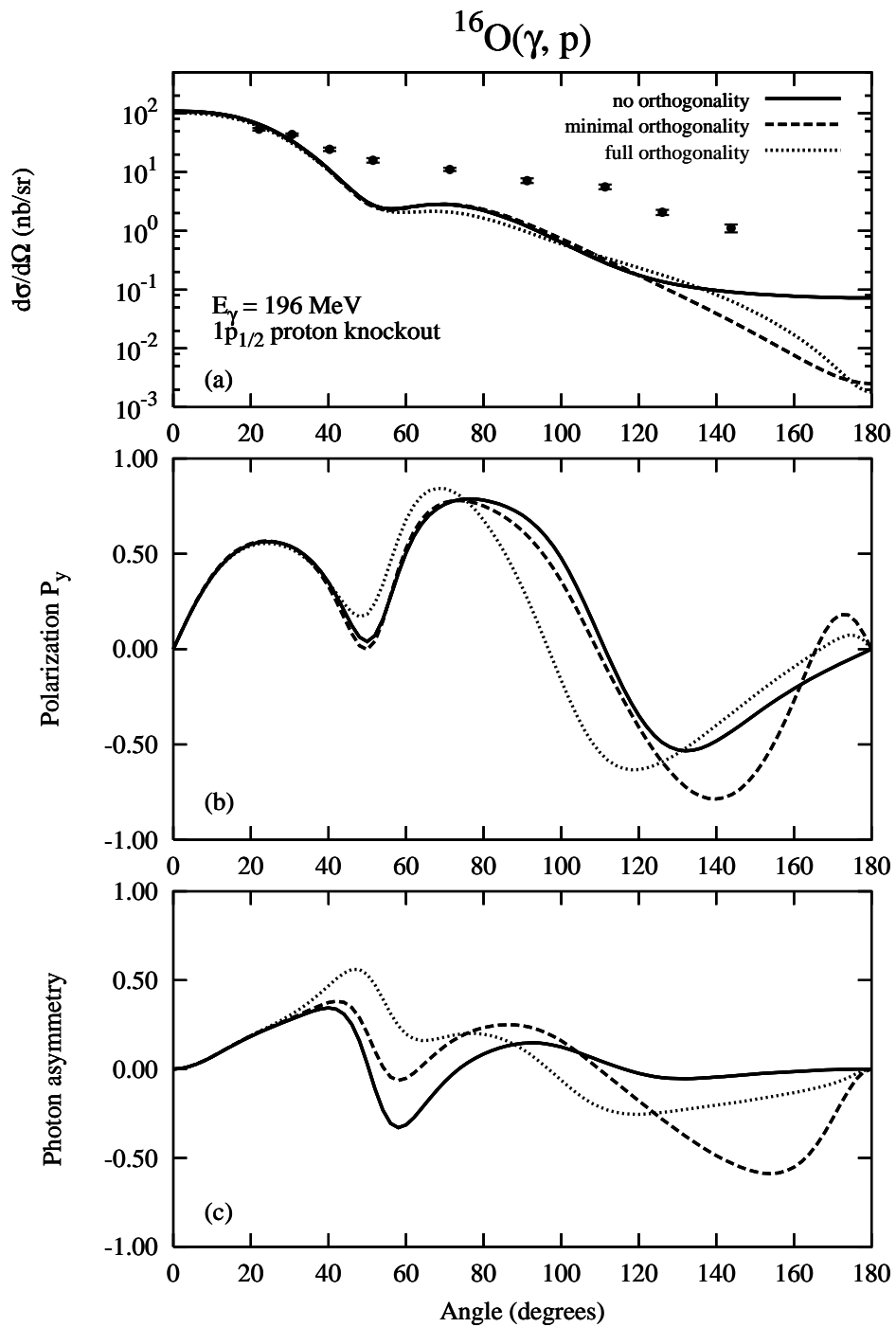


FIGURE 3

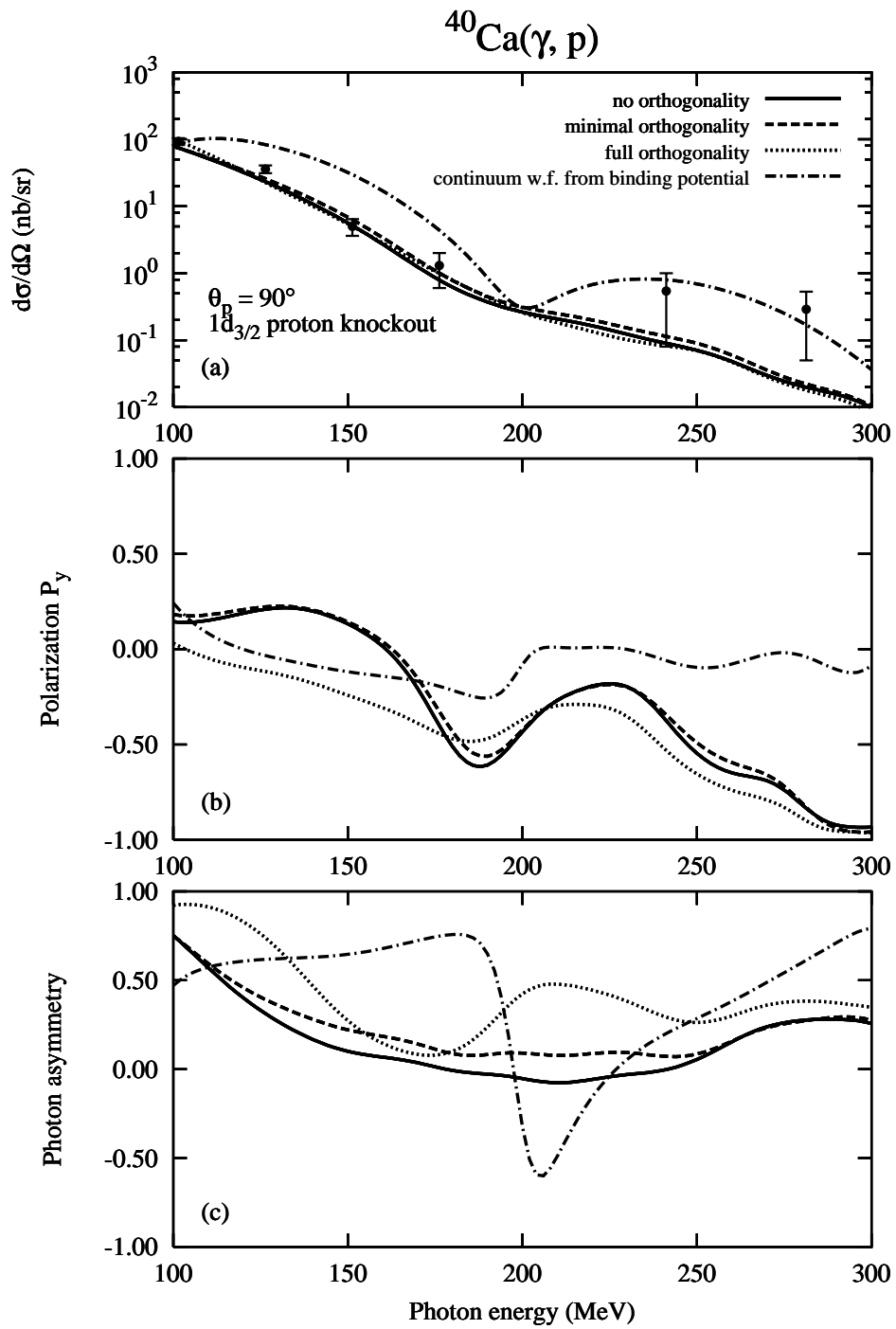


FIGURE 4

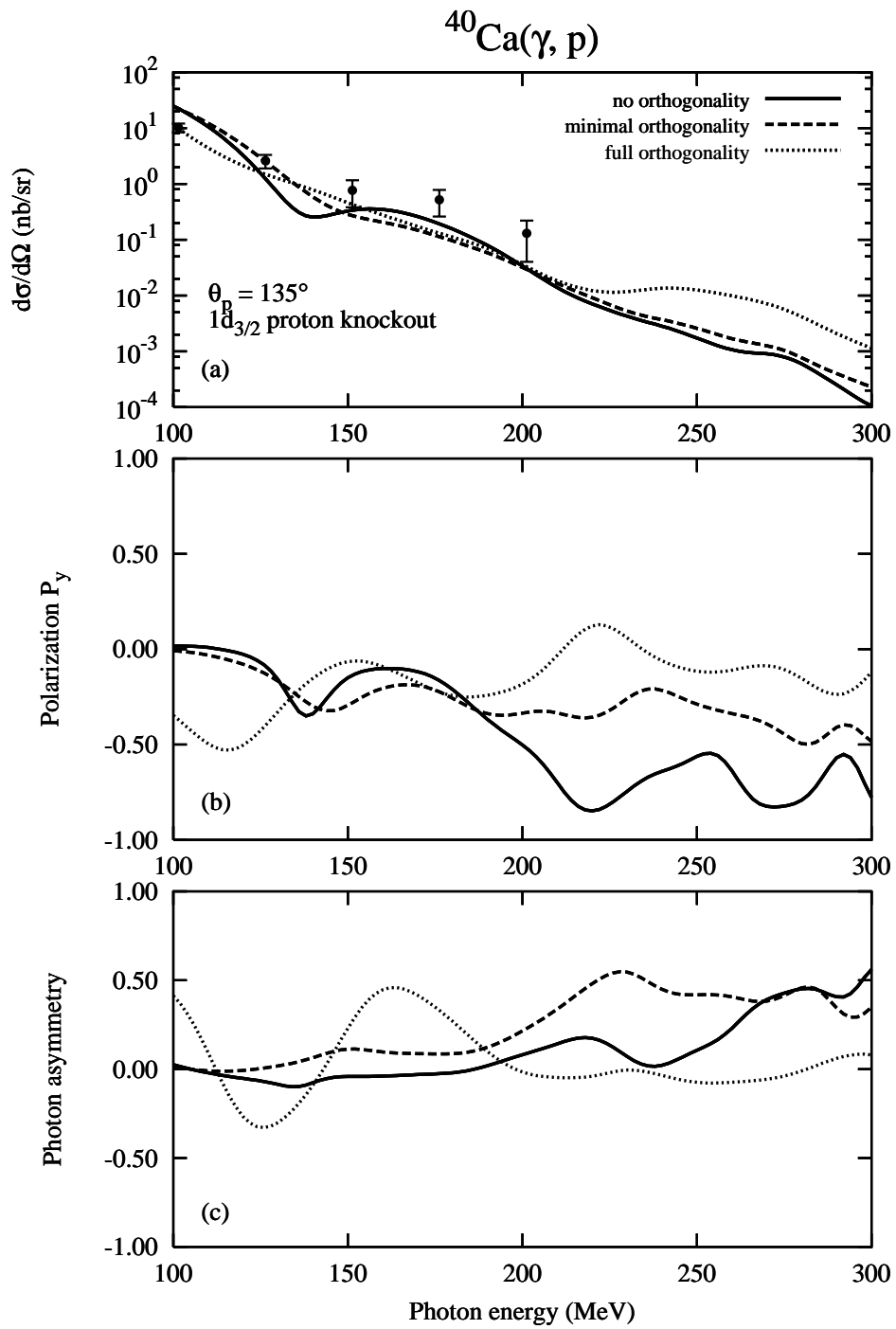


FIGURE 5

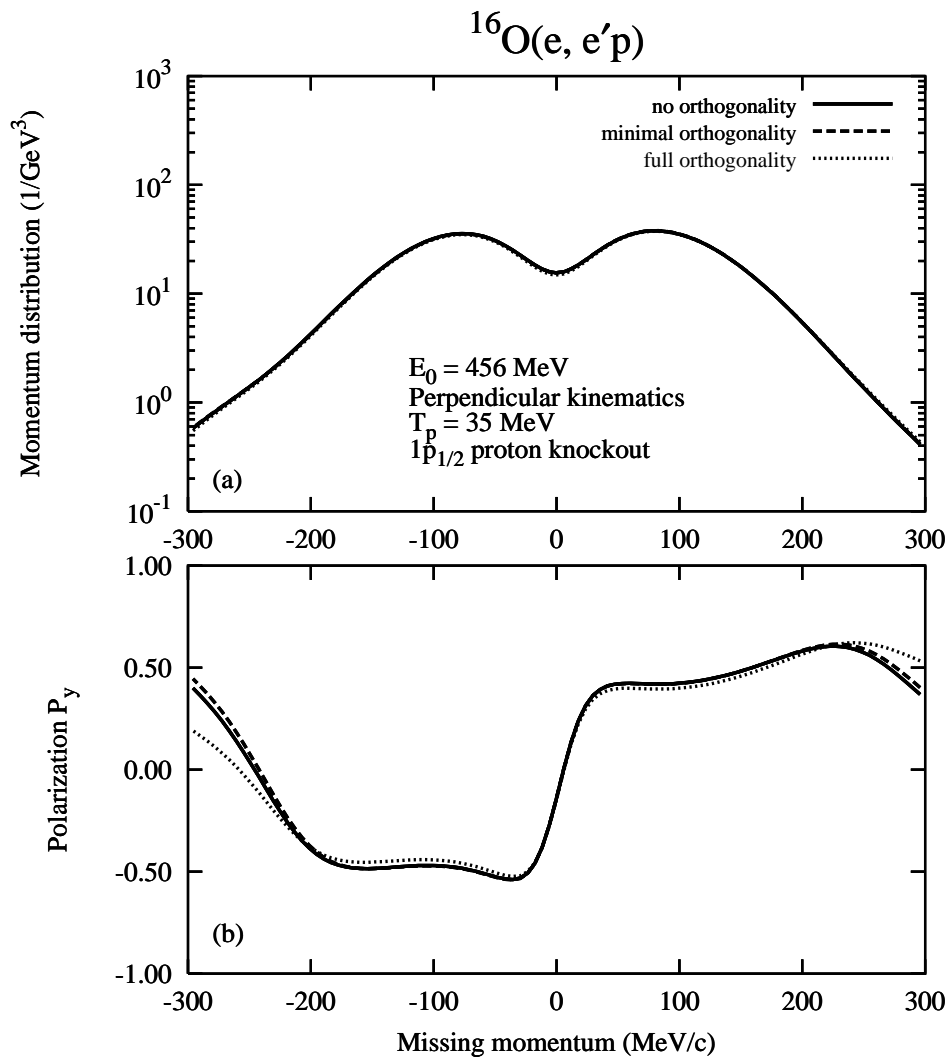


FIGURE 6

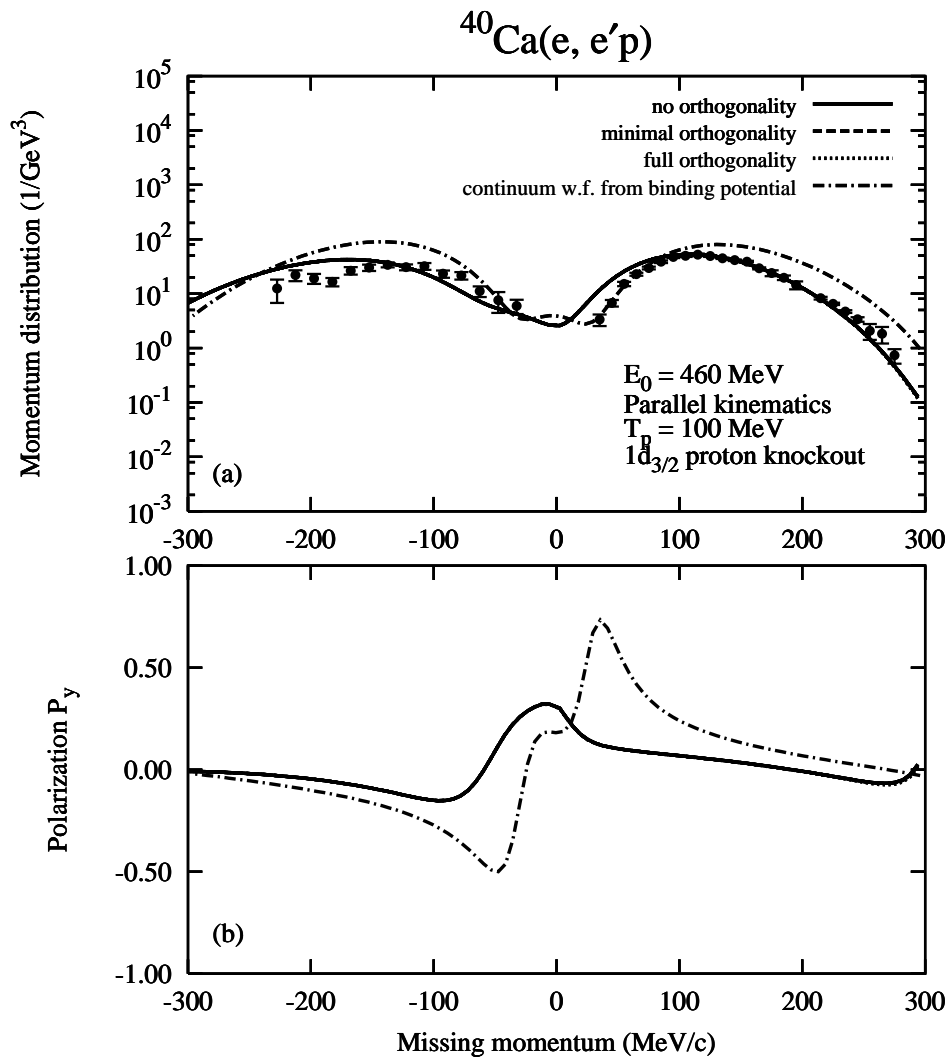


FIGURE 7